



<b>Publication Year</b>	2017
<b>Acceptance in OA @INAF</b>	2020-08-21T15:03:09Z
<b>Title</b>	Pulsation versus metallicity in Am stars as revealed by LAMOST and WASP
<b>Authors</b>	Smalley, B.; Antoci, V.; Holdsworth, D. L.; Kurtz, D. W.; Murphy, S. J.; et al.
<b>DOI</b>	10.1093/mnras/stw2903
<b>Handle</b>	<a href="http://hdl.handle.net/20.500.12386/26758">http://hdl.handle.net/20.500.12386/26758</a>
<b>Journal</b>	MONTHLY NOTICES OF THE ROYAL ASTRONOMICAL SOCIETY
<b>Number</b>	465

# Pulsation versus metallicity in Am stars as revealed by LAMOST and WASP

B. Smalley,<sup>1\*</sup> V. Antoci,<sup>2</sup> D. L. Holdsworth,<sup>3</sup> D. W. Kurtz,<sup>3</sup> S. J. Murphy,<sup>4,2</sup>  
P. De Cat,<sup>5</sup> D. R. Anderson,<sup>1</sup> G. Catanzaro,<sup>6</sup> A. Collier Cameron,<sup>7</sup>  
C. Hellier,<sup>1</sup> P. F. L. Maxted,<sup>1</sup> A. J. Norton,<sup>8</sup> D. Pollacco,<sup>9</sup>  
V. Ripepi,<sup>10</sup> R. G. West<sup>9</sup> and P. J. Wheatley<sup>9</sup>

<sup>1</sup>*Astrophysics Group, Lennard-Jones Laboratories, Keele University, Staffordshire ST5 5BG, UK*

<sup>2</sup>*Stellar Astrophysics Centre, Department of Physics and Astronomy, Aarhus University, DK-8000 Aarhus C, Denmark*

<sup>3</sup>*Jeremiah Horrocks Institute, University of Central Lancashire, Preston PR1 2HE, UK*

<sup>4</sup>*Sydney Institute for Astronomy (SIfA), School of Physics, The University of Sydney, NSW 2006, Australia*

<sup>5</sup>*Royal Observatory of Belgium, Av Circulaire 3-Ringlaan 3, B-1180 Brussels, Belgium*

<sup>6</sup>*INAF-Osservatorio Astrofisico di Catania, Via S. Sofia 78, I-95123 Catania, Italy*

<sup>7</sup>*SUPA, School of Physics and Astronomy, University of St Andrews, North Haugh, Fife KY16 9SS, UK*

<sup>8</sup>*Department of Physical Sciences, The Open University, Walton Hall, Milton Keynes MK7 6AA, UK*

<sup>9</sup>*Department of Physics, University of Warwick, Coventry CV4 7AL, UK*

<sup>10</sup>*INAF-Osservatorio Astronomico di Capodimonte, Via Moiriello 16, I-80131 Napoli, Italy*

Accepted 2016 November 6. Received 2016 November 6; in original form 2016 September 5

## ABSTRACT

We present the results of a study of a large sample of A and Am stars with spectral types from Large Sky Area Multi-Object Fiber Spectroscopic Telescope (LAMOST) and light curves from Wide Area Search for Planets (WASP). We find that, unlike normal A stars,  $\delta$  Sct pulsations in Am stars are mostly confined to the effective temperature range  $6900 < T_{\text{eff}} < 7600$  K. We find evidence that the incidence of pulsations in Am stars decreases with increasing metallicity (degree of chemical peculiarity). The maximum amplitude of the pulsations in Am stars does not appear to vary significantly with metallicity. The amplitude distributions of the principal pulsation frequencies for both A and Am stars appear very similar and agree with results obtained from *Kepler* photometry. We present evidence that suggests turbulent pressure is the main driving mechanism in pulsating Am stars, rather than the  $\kappa$ -mechanism, which is expected to be suppressed by gravitational settling in these stars.

**Key words:** asteroseismology – techniques: photometric – stars: chemically peculiar – stars: oscillations – stars: variables:  $\delta$  Scuti.

## 1 INTRODUCTION

The metallic-lined (Am) stars are a subset of the A-type stars that exhibit weak calcium K lines and enhanced iron-group spectral lines compared to their hydrogen-line spectral type (Titus & Morgan 1940; Roman, Morgan & Eggen 1948). They are further divided into *classical* and *marginal* Am stars. The spectral types obtained from the calcium K line ( $k$ ) and iron-group elements ( $m$ ) in classical Am stars differ by at least five spectral sub-types, whereas in the marginal Am stars the difference is less. There are also the ‘hot’ Am stars with spectral types around A0–A3, such as Sirius (Kohl 1964). As a group the Am stars rotate relatively slowly, which is thought to be a requisite condition for their chemical peculiarities

due to radiative diffusion (Michaud 1970). Many of the Am stars are in relatively short-period binary systems (Abt 1967; Carquillat & Prieur 2007; Smalley et al. 2014) and tidal synchronization is thought to be responsible for the observed low rotation rates in most Am stars (Abt & Moyd 1973; Wolff 1983). The results of the binarity studies indicate that there are some apparently single Am stars that were presumably born with slow rotation (Smalley et al. 2014; Balona et al. 2015a).

For many years, it was thought that classical Am stars did not pulsate (Breger 1970; Kurtz 1976) due to the gravitational settling of helium from the He II ionization zone where the  $\kappa$ -mechanism drives the pulsation of  $\delta$  Sct stars (e.g. Aerts, Christensen-Dalsgaard & Kurtz 2010). However, over time evidence emerged that some Am stars pulsate (e.g. Kurtz 1989; Henry & Fekel 2005). Recent studies using *Kepler* and Wide Area Search for Planets (WASP) photometry (Balona et al. 2011; Smalley et al. 2011) have found that a significant

\* E-mail: b.smalley@keele.ac.uk

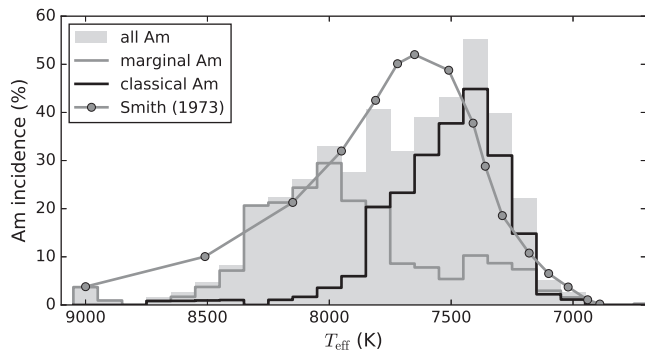


**Figure 1.** The percentage incidence of Am stars as a function of  $T_{\text{eff}}$ . The distribution given by Smith (1973) has been transformed from his  $b - y$  to  $T_{\text{eff}}$  using the  $uvby$  grids of Smalley & Kupka (1997).

fraction of Am stars do pulsate, but with a suspicion that they may do so at smaller amplitudes than the normal abundance  $\delta$  Sct stars.

The Large Sky Area Multi-Object Fiber Spectroscopic Telescope (LAMOST; Zhao et al. 2012) survey is providing a large catalogue of low-resolution stellar spectra. These are being automatically fitted to provide a homogeneous determination of stellar parameters for A, F, G and K stars: effective temperature ( $T_{\text{eff}}$ ) and surface gravity ( $\log g$ ) (Wu et al. 2011). Hou et al. (2015) presented a list of candidate Am stars using LAMOST data release 1 (DR1) spectra (Luo et al. 2015). From the 38 485 A and early-F stars in their LAMOST sample, they identified 3537 Am candidates and gave  $k$  and  $m$  spectral types.

The  $\Delta$  index presented by Hou et al. (2015) is defined as the numerical difference in the  $k$  and  $m$  spectral types. This value is used as the *metallicity* index in this study to separate classical Am stars from the marginal ones. Values of  $\Delta \geq 5$  are indicative of classical Am stars, while we use  $1 \leq \Delta < 5$  for marginal Am stars. Fig. 1 shows that the incidence of Am stars in this study as a function of  $T_{\text{eff}}$  is consistent with the earlier study of Smith (1973) and that the marginal and classical distributions are somewhat bimodal, with classical Am stars prevalent at lower temperature. As also seen in Smith (1973), the incidence of Am stars drops dramatically for stars cooler than  $T_{\text{eff}} \simeq 7000$  K.

In this work, we present the results of a search of the A and early-F stars in the LAMOST DR1, as used by Hou et al. (2015) in their search for Am stars, which have sufficient WASP (Pollacco et al. 2006) photometry to obtain the pulsation characteristics of the sample. The sample also allows for the investigation of pulsation incidence as a function of metallicity. In the context of this study, the A and early-F stars not listed as Am candidates will be referred to as ‘other A stars’ rather than ‘normal’ A and F stars, since the sample contains a contribution from other chemically peculiar stars, e.g. Ap and  $\lambda$  Boo stars (e.g. Wolff 1983).

## 2 SAMPLE SELECTION

The WASP project has been surveying the sky for transiting extra-solar planets using two robotic telescopes, one at the Observatorio del Roque de los Muchachos on the island of La Palma in the Canary Islands, and the other at the Sutherland Station, South African Astronomical Observatory. Both telescopes consist of an array of eight 200-mm,  $f/1.8$  Canon telephoto lenses and Andor CCDs, giving a field of view of  $7:8 \times 7:8$  and pixel size of around 14 arcsec. The observing strategy is such that each field is observed approximately every 10 min, on each observable night. WASP provides

good-quality photometry with a precision better than 1 per cent per observation in the approximate magnitude range  $9 \leq V \leq 12$ .

The WASP data reduction pipeline is described in detail in Pollacco et al. (2006). The aperture-extracted photometry from each camera on each night is corrected for primary and secondary extinction, instrumental colour response and system zero-point relative to a network of local secondary standards. The resultant pseudo- $V$  magnitudes are comparable to Tycho  $V$  magnitudes. Additional systematic errors affecting all the stars are identified and removed using the SYSREM algorithm of Tamuz, Mazeh & Zucker (2005).

For this study, the WASP archive was searched for light curves of stars with coordinates coincident with those of the LAMOST spectra to within 10 arcsec and with the requirement that at least 1000 photometric data points were available. Following the procedures of Smalley et al. (2011) and Holdsworth et al. (2014), amplitude spectra were calculated using the fast computation of the Lomb periodogram method of Press & Rybicki (1989) as implemented in the Numerical Recipes FASPER routine (Press et al. 1992). The periodograms were calculated covering the frequency range  $0-150 \text{ d}^{-1}$  for 30 282 stars in the LAMOST DR1 sample. Each periodogram was automatically searched for amplitude peaks with a signal-to-noise ratio (SNR) greater than 4 relative to the median background amplitude noise level and a false alarm probability (FAP) less than 0.1. For a peak to be deemed real, it must be present in more than one season of WASP photometry and have the same frequency to within the Rayleigh criterion ( $\sim 0.01 \text{ d}^{-1}$ ).

The diurnal gaps between successive observing nights introduce considerable sampling aliases in the amplitude spectra of most WASP light curves. Peaks which had a frequency within a Rayleigh criterion of the sidereal day frequency were rejected. Alias peaks due to frequencies  $n$  times the sidereal day frequency were also rejected, but with the Rayleigh criterion reduced by  $\sqrt{n}$ . This  $\sqrt{n}$  reduction was obtained empirically, based on an examination of all the peaks found in the sample, and models the diminishing frequency width of an alias peak above the background noise level as  $n$  increases. This considerably reduced the number of false-positive frequencies selected, but did not completely eliminate them. In addition, the same empirical relationship was used to remove the day aliasing of other found frequencies.

As the WASP pixels are relatively large, blending can be an issue, especially for fainter targets. By applying a requirement that no target shall be blended by more than 20 per cent within a 64 arcsec radius, the number of stars in the sample was reduced to 10 525, with 864 (9.3 per cent) being from the Hou et al. (2015) Am star list. The blending calculation was performed using the  $R$  magnitude photometry given in the Naval Observatory Merged Astrometric Dataset catalogue (Zacharias et al. 2004).

Of the 10 525 stars in our sample, around 1500 were identified as pulsation candidates. These were subjected to a separate more intensive analysis, involving a non-linear least-squares sinusoidal fit to the individual light curves, in order to obtain the frequencies and amplitudes of the signals present. In this work, the term amplitude refers to the semi-amplitude and not the peak-to-peak light variation. Up to a maximum of five frequency–amplitude pairs were selected; fewer if the FAP rose above 0.1. Finally, the stars were visually inspected with PERIOD04 (Lenz & Breger 2005) to confirm their variability characteristics.

The detection threshold for WASP data was estimated by Smalley et al. (2011) to be around 1 mmag. A more in-depth study by Holdsworth (2015) confirmed this and provided limits as a function of stellar magnitude. Fig. 2 shows the WASP median periodogram background noise at  $10 \text{ d}^{-1}$ , where the noise level is taken as the

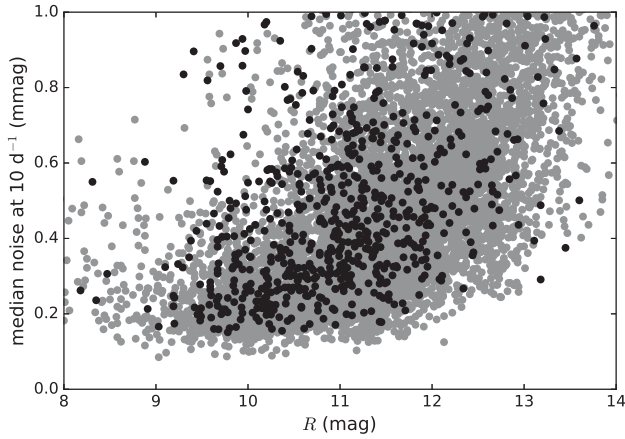


**Figure 2.** The WASP median periodogram background noise at  $10 \text{ d}^{-1}$  against  $R$  magnitude. The black dots are those stars found to pulsate, while the grey dots are those which were not found to pulsate.

median value of the periodogram within a bin of width  $1 \text{ d}^{-1}$ . Since our selection criterion for pulsations is that they must be present in at least two seasons of data, the seasons with the lowest noise levels are used and the noise values shown are the higher of these two. The requirement of  $\text{SNR} \geq 4$  indicates that the detection limit is at best  $0.6 \text{ mmag}$  for brighter stars, but varies significantly from star to star and falls off at the fainter end to above  $2 \text{ mmag}$ . Given that the LAMOST sample peaks around  $R = 11$ , a typical detection limit of no better than  $1 \text{ mmag}$  is expected, with a considerable tail.

### 3 RESULTS

The results from the frequency analysis are presented in Table 1. Several eclipsing binary systems were identified and labelled using the generic ‘EB’ label. The resistant mean method used to clean the WASP data to find pulsations has the side effect of removing deep eclipses from the light curves (Holdsworth et al. 2014). Stars were also labelled as being binary systems when a sub-harmonic of the principal frequency was found. Stars with low-frequency ( $\lesssim 2 \text{ d}^{-1}$ ) signals were investigated using PERIOD04 to ascertain whether the variations could be due to other physical causes, instead of ellipsoidal variations or pulsations. These were labelled as ‘Misc’ in Table 1. Often the classification of the variability is inconclusive in WASP data due to the noise level.

**Table 1.** The results of the search for variability in WASP light curves. In column 2,  $n$  is number of frequencies ( $f$ ) and peak amplitudes ( $a$ ) listed (up to 5). Column 5 gives the variable type inferred from the frequency analysis (see the text for details). Only the first 10 lines are shown here. The full 1193-line table is available online.

WASP ID	$n$	$f_1$ ( $\text{d}^{-1}$ )	$a_1$ (mmag)	Variable type	$f_2$ ( $\text{d}^{-1}$ )	$a_2$ (mmag)	$f_3$ ( $\text{d}^{-1}$ )	$a_3$ (mmag)	$f_4$ ( $\text{d}^{-1}$ )	$a_4$ (mmag)	$f_5$ ( $\text{d}^{-1}$ )	$a_5$ (mmag)
1SWASPJ000051.83+330532.9	1	35.4725	1.22	$\delta$ Sct								
1SWASPJ000246.71+160538.3	5	14.9049	2.83	$\delta$ Sct	17.8839	2.24	20.6246	1.97	14.7178	1.52	26.2976	1.32
1SWASPJ000331.13+123225.9	5	1.2281	9.12	$\gamma$ Dor	2.1342	7.42	1.1487	6.93	1.1140	5.13	1.2637	5.00
1SWASPJ000342.56+160511.0	2	3.8085	30.06	EB	1.9072	3.19						
1SWASPJ000444.67+304222.1	4	0.5579	5.33	$\gamma$ Dor	0.5666	4.51	0.6727	4.08	0.3887	3.64		
1SWASPJ000534.61+292745.0	1	15.8608	2.02	$\delta$ Sct								
1SWASPJ000613.54+362658.2	1	4.8405	65.22	$\delta$ Sct								
1SWASPJ000811.49+322128.7	4	0.4707	12.89	$\gamma$ Dor	0.6579	9.96	0.7926	9.01	0.6324	5.45		
1SWASPJ000924.89+031249.6	4	2.0414	10.18	$\gamma$ Dor	2.0879	5.90	1.9436	3.50	2.3354	2.53		
1SWASPJ001430.18+365226.0	2	4.6587	103.51	$\delta$ Sct	9.3189	17.68						

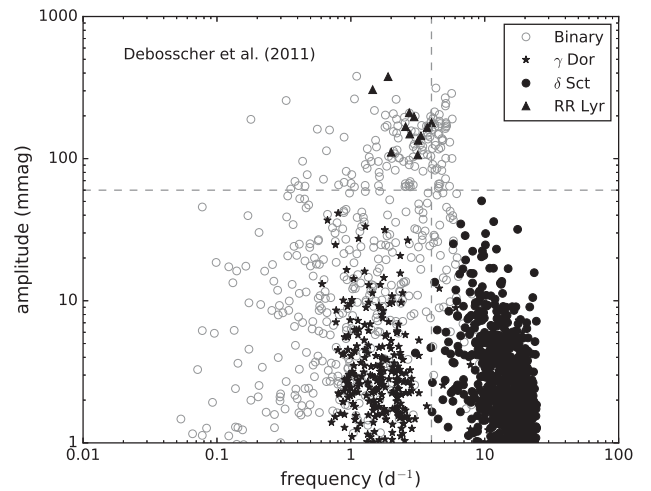
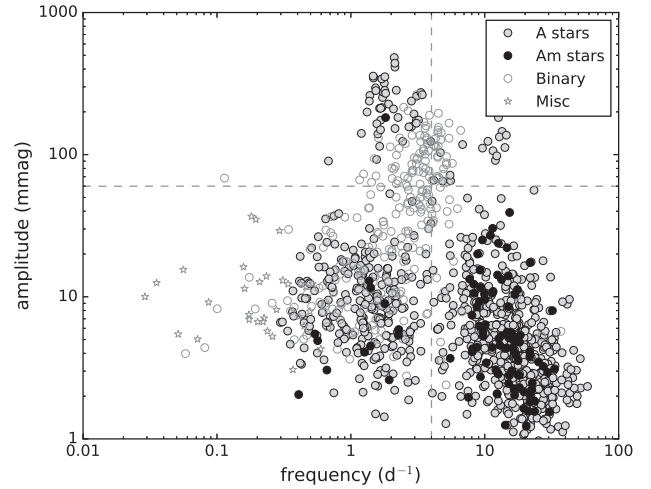


**Figure 3.** Frequency–amplitude diagram for the stars found to exhibit variability in the WASP photometry (top panel). The dashed lines indicate the four regions discussed in the text. The lower panel shows the *Kepler* results from Deboscher et al. (2011) for stars in the range  $6000 < T_{\text{eff}} < 10000 \text{ K}$  for comparison.

The frequency–amplitude distribution for the variable stars is shown in Fig. 3, with the *Kepler* results from Deboscher et al. (2011) for stars with temperatures in the range  $6000 < T_{\text{eff}} < 10000 \text{ K}$  shown for comparison. A frequency of  $5 \text{ d}^{-1}$  for the division between  $\delta$  Sct and  $\gamma$  Dor stars is sometimes used.

However, inspection of the WASP results suggests that  $4 \text{ d}^{-1}$  might be a better choice, as this corresponds to the minimum in the number of pulsators between the frequency domains where the two types mostly occur. Theory predicts that  $\gamma$  Dor stars rotating with 50 per cent of the critical velocity can have modes up to  $6 \text{ d}^{-1}$  (Bouabid et al. 2013). Nevertheless, while the choice of cutoff frequency is rather arbitrary, this study is concentrating on slow to moderately rotating stars, where Bouabid et al. (2013) predict a cutoff closer to  $4 \text{ d}^{-1}$ . An arbitrary upper amplitude limit for both  $\delta$  Sct and  $\gamma$  Dor stars was chosen, again by inspection of the WASP results, to be 60 mmag. Fig. 3 suggests that the location of Am pulsators does not appear to be different to that of the other A stars. There are several high-amplitude, low-frequency pulsators found which show the characteristics of RR Lyr stars (labelled ‘RRL’ in Table 1), plus a small group of higher amplitude  $\delta$  Sct stars (see Section 3.2).

To investigate the influence of atmospheric parameters on the pulsations, we further selected only those stars for which  $T_{\text{eff}}$  and  $\log g$  had been determined by LAMOST. Approximately 90 per cent of the original sample have stellar parameters, which reduced the number in the final sample to 9219, with 808 of them being Am stars. The uncertainties in  $T_{\text{eff}}$  and  $\log g$  have average values of  $\pm 135 \text{ K}$  and  $\pm 0.43 \text{ dex}$ , respectively. The quoted uncertainty in  $\log g$  could possibly be overestimated as it is much larger than the scatter in the values in the current sample. In addition, the quoted uncertainties could be larger due to the presence of binary systems. This will mostly affect systems with moderately dissimilar components and modest brightness ratios, since for nearly equal stars and those with large brightness ratios the effect will be minimal.

The location of Am and the other A stars in the  $T_{\text{eff}}\text{--}\log g$  plane is shown in Fig. 4. The pulsating Am stars are mostly located within the temperature range  $6900 < T_{\text{eff}} < 7600 \text{ K}$ , which is towards the red edge of the  $\delta$  Sct instability strip. Note that this region is also dominated by the classical Am stars. At higher temperatures, the decline in pulsating Am stars appears to occur around the blue edge of the  $\gamma$  Dor instability strip, but this could be coincidence. In contrast, the other A star population of  $\delta$  Sct pulsators extends to much hotter temperatures.

### 3.1 $\gamma$ Dor pulsations

There are relatively few  $\gamma$  Dor Am pulsators in the WASP sample. With the exception of one possibly misclassified star, they are all to be found within the ground-based  $\gamma$  Dor instability strip. This region also contains the majority of the  $\delta$  Sct Am stars, which suggests that they are probably hybrids (see Section 4.3). However, it is not clear whether the low numbers are related purely to temperature, or if there is interplay between peculiarity and g-mode pulsation. The incidence of Am stars exhibiting  $\gamma$  Dor pulsations is roughly half that of the other A stars. However, the lack of many  $\gamma$  Dor Am pulsators is consistent with the relative low number of Am stars in the region where pure g-mode  $\gamma$  Dor pulsators predominately occur. The convective envelopes of  $\gamma$  Dor stars are, on average, deeper than those of  $\delta$  Sct stars and mixing by convective motions causes the peculiarities to vanish. The  $\gamma$  Dor pulsators have frequencies in the range where WASP data are most significantly affected by the diurnal sampling. Therefore, we will not consider these stars any further in the current work.

### 3.2 Higher amplitude pulsations

As mentioned earlier, we identified a small group of  $\delta$  Sct stars with amplitudes  $>60 \text{ mmag}$ . In the temperature range  $6900 < T_{\text{eff}} <$

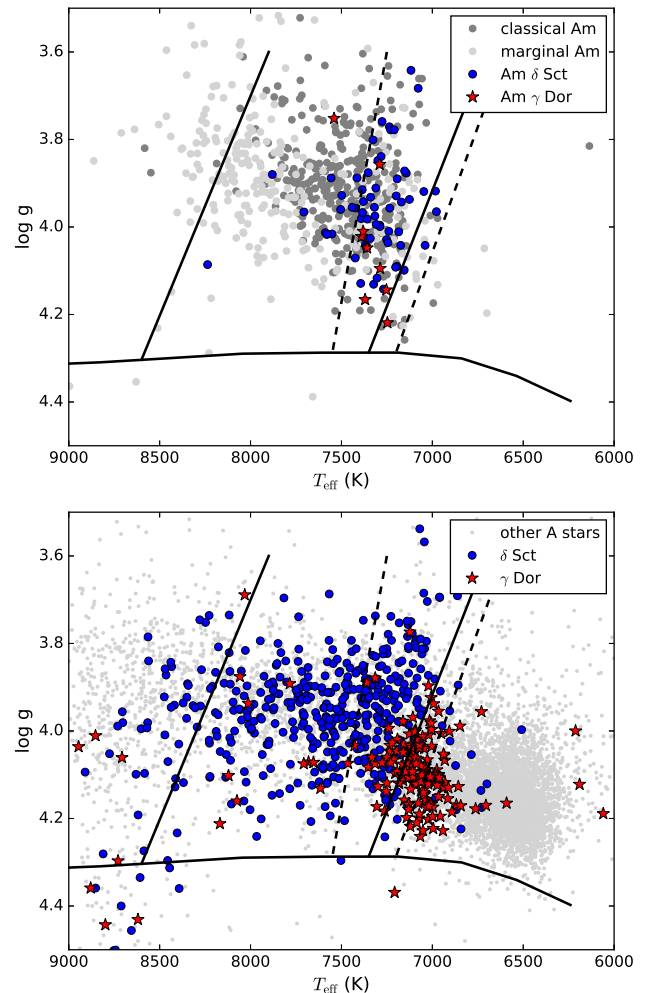


**Figure 4.** Temperature–gravity diagrams showing the location of Am stars (top panel) and other A stars (bottom panel) in the LAMOST-WASP sample. The location of the identified  $\delta$  Sct and  $\gamma$  Dor pulsators is also shown. The locations of the ground-based  $\delta$  Sct (solid line; Rodríguez & Breger 2001) and  $\gamma$  Dor (dotted line; Handler & Shobbrook 2002) instability strips are shown, together with the ZAMS (near-horizontal solid line).

7600 K there are only 10 of these stars, but none of them have been classified as Am stars. Randomly picking 10 stars from the WASP sample, using the hypergeometric probability distribution (Spiegel, Schiller & Srinivasan 2001), predicts an average of  $1.8 \pm 1.2$  Am stars being selected and the probability of not picking any Am stars is 14 per cent. It is, therefore, possible that the lack of Am stars in this small group could be due to a sampling effect. Indeed, the lack of any such stars in the Debosscher et al. (2011) results presented in the bottom panel of Fig. 3 shows that these are not common among the  $\delta$  Sct stars in general. However, we cannot exclude the possibility that there are no Am stars in this region due to physical mechanisms preventing either the peculiarities or the oscillations from occurring.

Most RR Lyr stars have  $T_{\text{eff}} < 6900 \text{ K}$  and are therefore too cool to be considered in the discussion of Am stars. In the WASP sample of RR Lyr stars there are only four hotter than 6900 K. There is one Am candidate found in the RR Lyr domain, AL CMi, but it has no LAMOST stellar parameters. Literature broad-band photometry of this star suggests that  $T_{\text{eff}} \simeq 7000 \text{ K}$ , putting this star within the realm of the Am stars. Layden (1994) determined a metallicity of

$[M/H] = -0.85$  for AL CMi. However, this was determined from the relative strengths of the Ca K and the Balmer lines and indicates that the calcium line is significantly weaker than expected. The weak Ca K line has resulted in Hou et al. (2015) misclassifying this RR Lyr star as a classical Am star.

### 3.3 Binarity

Brightness variations consistent with being binary systems were found for 249 stars in the WASP sample. The majority appear to show ellipsoidal variations with periods  $\lesssim 3$  d, while a few have Algol-like eclipses. Of the 249 binary stars, 26 also exhibit  $\delta$  Sct pulsations, but none is an Am star. However, there are only 11 Am stars among the 249 binary systems. Previously, in their analysis of 1742 Am stars, Smalley et al. (2014) found that only 4 out of 70 ( $\sim 6$  per cent) eclipsing binary systems found also had a pulsating component detectable with WASP. The fact that pulsations have not been detected in the 11 Am stars in the current WASP sample is not statistically significant. In this work, we have not performed an in-depth search for eclipsing binary systems in the WASP light curves and, therefore, will not consider this any further.

## 4 $\delta$ SCT PULSATIONS

In this study, we concentrate on the stars with  $\delta$  Sct pulsations. These are selected as having their principal pulsation frequency  $> 4$  d $^{-1}$  and an amplitude  $< 60$  mmag. Inspection of Fig. 3 reveals that there is a lack of Am stars with principal frequencies above 40 d $^{-1}$ , while the Smalley et al. (2011) results do contain some Am stars with higher frequencies. However, this is a selection effect, as the higher frequency pulsations tend to be found in hotter stars (Rodríguez, López-González & López de Coca 2000). All stars in the WASP sample with principal frequency  $> 40$  d $^{-1}$  have  $T_{\text{eff}} \gtrsim 7800$  K, which is hotter than where most of the classical Am stars are located. Furthermore, in Smalley et al. (2011) the high-frequency pulsators all appear to be hotter stars. This was also the case in Holdsworth et al. (2014), where 12 of 13 high-frequency pulsating Am stars had  $T_{\text{eff}} > 7600$  K, with 11 having  $T_{\text{eff}} \geq 7800$  K.

The location of the majority of the Am star pulsators is restricted to the temperature range  $6900 < T_{\text{eff}} < 7600$  K. The  $\delta$  Sct pulsators among the other A stars show a wider distribution of effective temperatures, especially to hotter temperatures. Clearly, there is a difference between the temperature distributions of pulsating Am stars and pulsating other A stars. Splitting the Am stars into classical and marginal, using the  $\Delta$  index, reveals that the classical Am stars are concentrated towards the red edge of the  $\delta$  Sct instability strip, while the marginal Am stars are more spread and peak at slightly hotter temperatures (Fig. 1). The  $\Delta$  index is also sensitive to temperature, since the Ca K line lies on the flat part of the curve of growth (Kurtz 1978). Therefore, the marginal Am stars also contain a contribution from the hot Am stars that may have high abundance anomalies, but these do not show as strongly in spectroscopic classification criteria at higher temperatures. In the temperature range  $6900 < T_{\text{eff}} < 7600$  K around 13 per cent of the classical Am stars have been found to pulsate, while for the marginal Am stars this rises to around 24 per cent.

### 4.1 Variation with metallicity

The location of Am pulsators is almost exclusively confined to the region with  $T_{\text{eff}}$  cooler than  $\sim 7600$  K (Fig. 5). With very few exceptions, there is no significant variation in the  $T_{\text{eff}}$  range with

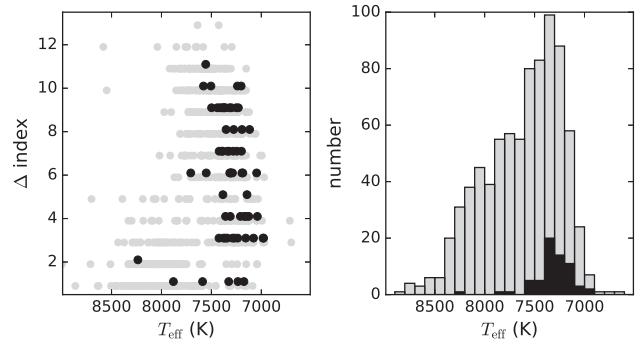


**Figure 5.** The location of Am stars within the  $T_{\text{eff}}-\Delta$  plane (left-hand panel). The light grey filled circles are the Am stars and the black filled circles are those found to exhibit  $\delta$  Sct pulsations. Note that the different symbols have been offset slightly in  $\Delta$  for clarity. Irrespective of metallicity the Am pulsators are mostly confined to the region with  $T_{\text{eff}}$  cooler than  $\sim 7600$  K. The right-hand panel shows the incidence of Am stars as a function of  $T_{\text{eff}}$  (light grey histogram), along with those found to pulsate (black histogram). The histogram bin width is 100 K.

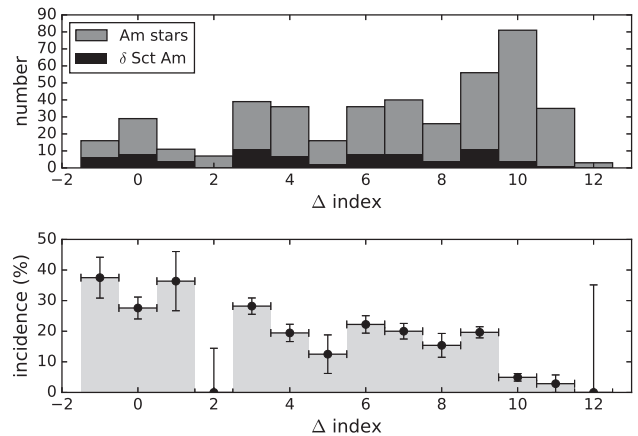


**Figure 6.** The variation of pulsation in Am stars as a function of metallicity index ( $\Delta$ ). The top panel shows the number of Am stars per  $\Delta$  index bin (grey bars) and the number exhibiting  $\delta$  Sct pulsations (black bars). The lower panel shows the incidence of the Am pulsations. The error bars indicate the width of the  $\Delta$  index bin and the uncertainty in the incidence caused by the discrete nature of the small numbers per bin. In both panels, the temperature range is restricted to  $6900 < T_{\text{eff}} < 7600$  K.

metallicity. Hence, the location of Am pulsators appears to be strongly determined by  $T_{\text{eff}}$  and not significantly dependent on metallicity.

There are 76 Am stars identified as having  $\delta$  Sct pulsations out of a total of 439 Am stars within the temperature range  $6900 < T_{\text{eff}} < 7600$  K, giving an overall incidence for pulsating Am stars of 17 per cent. Fig. 6 shows the variation in the incidence of pulsating Am stars versus  $\Delta$  index. There is a distinct trend with  $\Delta$  index, with the incidence of pulsations decreasing as the metallicity increases. Both Pearson ( $-0.71$ ) and Spearman ( $-0.67$ ) correlation coefficients indicate strong negative correlations, with confidences  $> 99$  per cent. We, therefore, conclude that classical Am stars are less likely to exhibit  $\delta$  Sct pulsations than marginal Am stars at the precision of the WASP photometry.

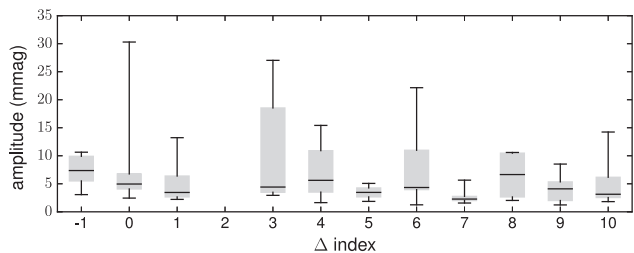


**Figure 7.** The variation of principal pulsation amplitude as a function of metallicity index ( $\Delta$ ). The boxes extend from the lower to upper quartile amplitude with the horizontal lines indicating the median, and the whiskers extending from the box give the full amplitude range. The temperature range is restricted to  $6900 < T_{\text{eff}} < 7600$  K.

#### 4.2 Lower amplitudes in Am stars?

The results of previous investigations into Am pulsations have led to a suspicion that they have lower amplitudes than normal  $\delta$  Sct stars (Smalley et al. 2011). Fig. 7 shows that there is no obvious trend in principal pulsation amplitude with  $\Delta$ . There does not appear to be any significant difference in the pulsation amplitudes of classical Am stars compared to those of the marginal Am stars. The maximum amplitude for pulsating Am stars is also not significantly different from that of the other A stars. Hence, at the millimagnitude precision of the WASP data, there is no evidence to support the notion that Am stars might have lower pulsation amplitudes than other  $\delta$  Sct stars.

In their analysis of 29 Am stars observed by *Kepler* and *K2* Campaign 0, Balona et al. (2015a) identified 12 stars with  $\delta$  Sct pulsations. Of these, five have at least one pulsation amplitude above 1 mmag and, therefore, potentially detectable by WASP. The incidence rate (17 per cent) is consistent with that found in the current study. The remaining seven stars, however, have amplitudes too low to be detectable by WASP. The distribution of the pulsation amplitudes for the general population of  $\delta$  Sct stars identified by Debosscher et al. (2011) has  $\sim 60$  per cent with amplitudes above 1 mmag. Hence, this percentage implies that the probability of selecting seven or more stars out of 12 with amplitudes  $< 1$  mmag is 16 per cent. Therefore, this small sample does not provide strong significant evidence to support the hypothesis that pulsation amplitudes of Am stars might be systematically lower than those of the general population of  $\delta$  Sct stars.

To investigate this further, we have extended the sample of Am stars with *Kepler/K2* photometry as follows. The Hou et al. (2015) list of Am stars includes 67 with *Kepler* photometry. These are principally from the LAMOST-*Kepler* project (De Cat et al. 2015). The *Kepler* Presearch Data Conditioning (Jenkins et al. 2010) light curves of these, together with the Balona et al. (2015a) stars, were analysed with `PERIOD04` to obtain their principal pulsation frequency and amplitude.

In addition, *K2* has observed further Am stars from the catalogue of Renson & Manfroid (2009) during Campaigns 1 to 4.<sup>1</sup> Further inspection of the Hou et al. (2015) list revealed that 16 and 5 Am stars were also observed during Campaigns 0 and 4, respectively. The *K2* light curves, extracted using the *K2P<sup>2</sup>* pipeline (Lund et al. 2015),<sup>2</sup> were also examined using `PERIOD04`.

<sup>1</sup> *K2* Guest Observer programs: GO1014, GO2012, GO3012, GO4045; all P.I. B. Smalley.

<sup>2</sup> Available from the *Kepler* Asteroseismic Science Operations Centre; <http://kasoc.phys.au.dk>.

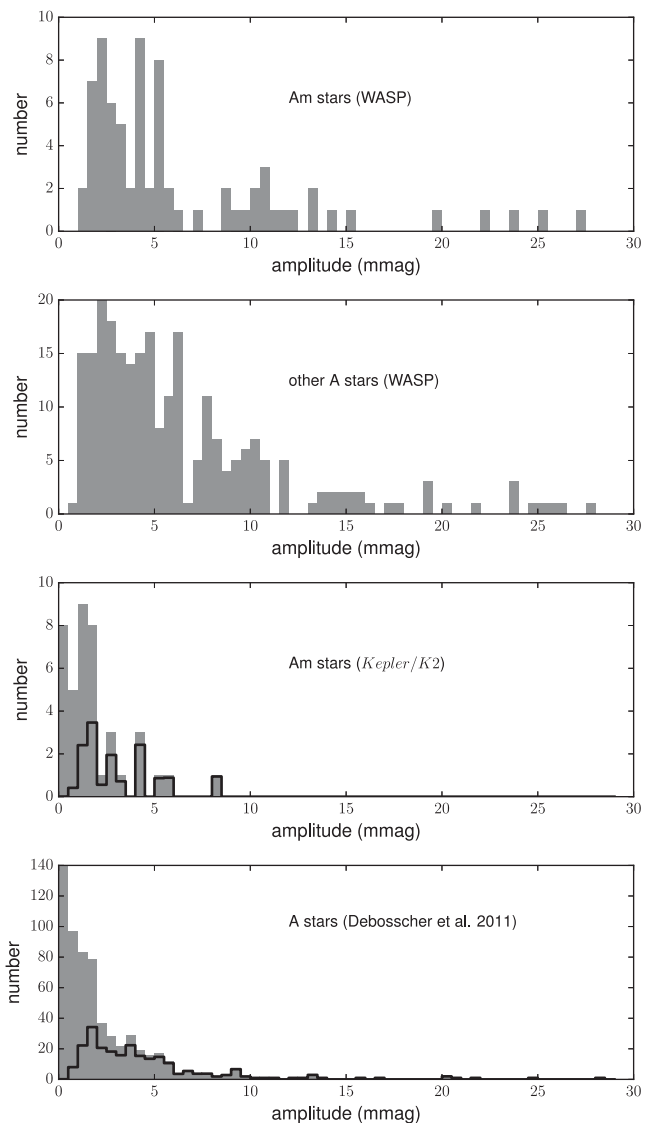


**Figure 8.** The pulsation amplitude distributions for Am and other A stars from WASP (upper two panels) and *Kepler/K2* (lower two panels). These are presented as solid grey histograms with bin sizes of 0.5 mmag. In the lower two panels, the outline histogram shows the amplitude distribution after being convolved with the WASP observability function to simulate the expected WASP amplitude distribution. Note the different ordinate scales for the panels.

In total, 144 Am stars were observed by *Kepler* and *K2*. Of these, 42 ( $\sim 30$  per cent) have principal pulsation frequencies and amplitudes within the  $\delta$  Sct range and 29 stars have amplitudes above 1 mmag. The fraction of pulsating Am stars with amplitudes greater than 1 mmag is 64 per cent, which is consistent with that obtained above from the Debosscher et al. (2011) sample of  $\delta$  Sct stars. Furthermore, approximately 20 per cent of the Am stars have pulsations with amplitudes detectable by WASP, which is compatible with the incidence rate found in the current study. There is, however, a lack of Am pulsators with amplitudes above 10 mmag, but this could be due to the relatively low number of pulsators in the *Kepler/K2* sample.

The amplitude distributions of the Am and other A stars from the WASP and *Kepler/K2* samples are shown in Fig. 8. The amplitude distributions for the Am and other A stars are broadly similar. In

order to ascertain whether the WASP amplitude distributions are consistent with that found from the space-based *Kepler/K2* photometry, a WASP observability function was generated from the distribution of the WASP median noise background measurements (see Fig. 2) and the  $\text{SNR} = 4$  selection criterion. The observability function was convolved with the Debusscher et al. (2011) and *Kepler/K2* amplitude distributions in order to predict the amplitude distributions for the Am and other A star pulsators expected from the WASP sample. It is evident from Fig. 8 that the observed and expected WASP distributions for the Am and other A stars are indeed similar.

### 4.3 Hybrids

There are several stars for which both  $\delta$  Sct and  $\gamma$  Dor frequencies were detected in the WASP light curves. There are 8 Am and 24 other A stars with LAMOST stellar parameters in the temperature range  $6900 < T_{\text{eff}} < 7600$  K. They are spread around the  $T_{\text{eff}}\text{-}\log g$  plane within the area occupied by the other pulsators and not concentrated in any particular region. If these hybrid pulsators are spread equally among the stars in the above  $T_{\text{eff}}$  range, then there is a 20 per cent probability that at least eight of them will be Am stars.

In their analysis of early *Kepler* data, Grigahcène et al. (2010) suggested that hybrid pulsators might be more common among the Am stars. However, a later study by Balona, Daszyńska-Daszkiewicz & Pamyatnykh (2015b) did not support this suggestion, finding that at *Kepler* precision hybrid pulsators are very common. Of the eight Am stars with hybrid pulsations, five are classical and three are marginal. Picking eight stars at random from the 387 Am stars in the temperature range  $6900 < T_{\text{eff}} < 7600$  K results in a 74 per cent probability of at least five classical Am stars being selected. However, the number of hybrids found in this work is rather too low to provide meaningful statistics.

## 5 PULSATION MODELLING

In their analysis of the pulsating Am star HD 187547, Antoci et al. (2014) suggested that turbulent pressure is responsible for a large part of the excitation in the H/He I ionization layer. Using non-adiabatic pulsational stability analyses (Balmforth 1992; Houdek et al. 1999) with time-dependent non-local convection treatment models (Gough 1977a,b), the authors found that only the lowest radial orders were excited by the  $\kappa$ -mechanism in the He II ionization layer. Surprisingly, most pulsation modes were driven by the turbulent pressure in the H/He I layer and not in the He II ionization layer. Furthermore, oscillations can be excited by turbulent pressure acting in the H/He I ionization layer, without any contribution from the  $\kappa$ -mechanism. These findings are compatible with pulsations in many Am stars, which otherwise remain unexplained.

Using the models described above, we show non-adiabatic pulsational stability analyses of a star with global stellar parameters representative of Am stars:  $M = 2.3 M_{\odot}$ ,  $T_{\text{eff}} = 7500$  K,  $L = 25.7 L_{\odot}$ . The non-local convection parameters  $a$ ,  $b$  and  $c$  for the theory of Gough (1977a) were chosen to be  $a^2 = b^2 = c^2 = 950$ . We used the OPAL opacity tables (Rogers & Iglesias 1995) supplemented by the Ferguson et al. (2005) tables at low temperatures. It is beyond the scope of the current work to go into details concerning the theoretical aspect of mode stability, but for details we refer the reader to Houdek et al. (1999) and Antoci et al. (2014).

In Fig. 9, we show the normalized growth rates ( $\eta/\omega_r$ , where  $\eta$  and  $\omega_r$  are, respectively, the imaginary and real parts of the eigenfrequency) as a function of frequency. Whenever  $\eta/\omega_r > 0$ , the

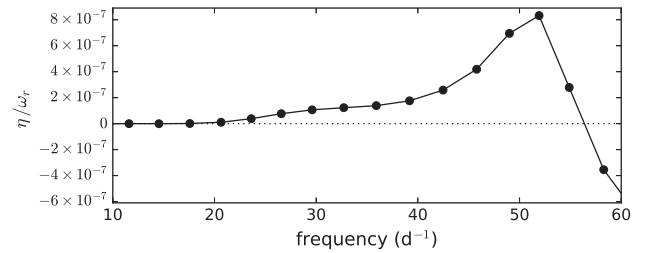


**Figure 9.** Normalized growth rate ( $\eta/\omega_r$ ) as a function of frequency for the model described in the text. A positive growth rate indicates excited pulsation modes, while a negative value indicates damped modes.

pulsation mode is intrinsically excited and  $\eta/\omega_r < 0$  indicates an intrinsically damped mode. To further illustrate the driving agent of these modes, we show the accumulated work integrals as a function of total pressure for four different radial orders (Fig. 10). The continuous lines depict the total accumulated work integral, which when positive at the stellar surface means that the mode is intrinsically excited. The dashed and dotted lines reflect the contribution of turbulent and gas pressure, respectively, to the total accumulated work integral. The grey areas depict the H/He I and the He II ionization layers and correspond to the convection zones in a star with the parameters outlined above. Note, however, that these zones are likely linked through overshooting and that additional convection zones may occur deeper into the star due to atomic diffusion (e.g. Théado et al. 2012; Deal, Richard & Vauclair 2016).

As illustrated in Fig. 10, the radial fundamental mode (order 1) is damped because the total accumulated work integral is not positive. There is some driving due to gas pressure in the He II ionization layer; however, the mode is damped in the H/He I layer. The fourth radial order mode, on the other hand, is intrinsically excited by gas pressure in the He II layer. This is illustrated by the local increase on the accumulated work integral. Also, in this case, turbulent pressure has a slight damping effect on the mode. The seventh radial order mode is clearly intrinsically excited by both, turbulent and gas pressure in the H/He I and He II layers, respectively. For the 10th radial order mode; however, the excitation predominantly occurs due to the turbulent pressure in the H/He I ionization layer.

In order to conclude whether turbulent pressure can fully explain the phenomenon of pulsation in Am stars, a more global study covering the entire instability strip is required (Antoci et al., in preparation). The current model does not include the diffusion of He. Adding He depletion increases the range of excited modes, which will be explored in detail in the forthcoming study. Nevertheless, there are strong indications that both turbulent pressure and excitation reach a maximum around 7500 K (Antoci et al. 2014; Grassitelli et al. 2015), which is in the region where pulsating Am stars are found in our study.

## 6 DISCUSSION AND CONCLUSION

From a large sample of A and Am stars observed with LAMOST and WASP, we have found that  $\delta$  Sct pulsations in Am stars are mostly confined to a region close to the red edge of the  $\delta$  Sct instability strip. Their location is generally within the temperature range  $6900 < T_{\text{eff}} < 7600$  K and is independent of metallicity. The incidence of pulsations in Am stars decreases noticeably in more peculiar Am stars. The reason for the decrease is not known, but we might expect the  $\kappa$ -mechanism and turbulent pressure to interact depending on several parameters, including the diffusion of helium, stellar mass and evolutionary stage, as well as the global



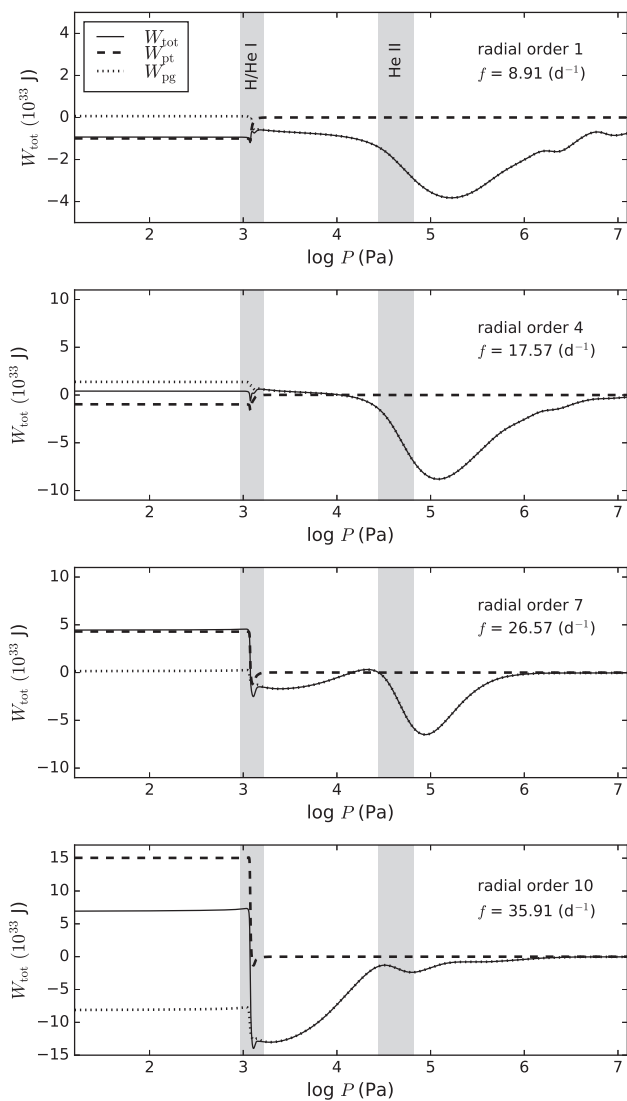


**Figure 10.** The accumulated work integrals ( $W_{\text{tot}}$ ) as a function of total pressure ( $\log P$ ) for four different radial orders. The continuous lines depict the total accumulated work integral, which when positive at the stellar surface means that the pulsation mode is intrinsically excited. As shown in the top panel, the dashed and dotted lines reflect the contribution of turbulent ( $W_{\text{pt}}$ ) and gas ( $W_{\text{pg}}$ ) pressure, respectively, to the total accumulated work integral. As indicated in the top panel, the grey areas depict the H/He I and the He II ionization layers and correspond to the convection zones in a star.

metallicity. Nevertheless, the observations presented in the current work are consistent with the hypothesis proposed by Murphy (2014) that the non-pulsating stars in the  $\delta$  Sct instability strip are Am stars. The amplitudes of pulsations found with WASP agree with expectations based on the results from *Kepler*. There is some, albeit rather weak, evidence for lower amplitudes for Am pulsators compared to other A stars.

The mystery of why Am stars pulsate (or at least some of them) originates from the assumption that it is the  $\kappa$ -mechanism operating in the He II ionization layer that excites  $\delta$  Sct oscillations. The blue edge of the  $\delta$  Sct instability strip moves redward as helium abundance is reduced, while the red edges remain almost constant (Cox, Hodson & King 1979; Turcotte et al. 2000; Xiong, Deng & Wang 2015). This is consistent with the location of pulsating Am stars found in our study. However, the lack of any significant cor-

relation of location and amplitude with metallicity suggests that another mechanism may be at play. We would expect that as metallicity increases and, by inference, helium abundance in the He II ionization layer decreases, the location of pulsating Am stars should be further marginalized to cooler temperatures.

In pulsating Am stars, we suggest that a large part of the excitation occurring in the H/He I ionization layer is driven by turbulent pressure. Low radial order modes in normal  $\delta$  Sct stars are excited by the  $\kappa$ -mechanism. However, the higher ones are predominantly driven by turbulent pressure in a temperature-dependent manner, since turbulent pressure damps oscillations in stars close to the red edge of the  $\delta$  Sct instability strip. While the WASP data in this work indicate that Am and normal  $\delta$  Sct stars do not show oscillations with frequencies higher than around  $30 \text{ d}^{-1}$ , we know from other WASP and *Kepler* studies that there are Am and non-Am  $\delta$  Sct stars showing pulsations up to  $80\text{--}90 \text{ d}^{-1}$ . For example, HD 187547 is an Am star with pulsations covering a frequency range from 20 to  $80 \text{ d}^{-1}$  (Antoci et al. 2014). The amplitudes of the highest radial order modes are lower than 0.15 mmag. WASP could not detect these amplitudes. We conclude that it is plausible that Am stars have on average higher radial order modes excited due to the turbulent pressure being more efficient as the depleted He is offset by an increase in hydrogen number density.

## ACKNOWLEDGEMENTS

The WASP project is funded and operated by Queen’s University Belfast, the Universities of Keele, St Andrews and Leicester, the Open University, the Isaac Newton Group, the Instituto de Astrofísica de Canarias, the South African Astronomical Observatory and by the UK Science and Technology Facilities Council (STFC). Funding for the Stellar Astrophysics Centre was provided by the Danish National Research Foundation (grant no. DNR106). The research is supported by the ASTERISK project (ASTERoseismic Investigations with SONG and Kepler) funded by the European Research Council (grant agreement no. 267864). DWK is supported by the STFC. DLH acknowledges support from the STFC via grant number ST/M000877/1. SJM was supported by the Australian Research Council.

## REFERENCES

- Abt H. A., 1967, in Cameron R. C., ed., *Magnetic and Related Stars*. Mono Book Corporation, Baltimore, p. 173  
 Abt H. A., Moyd K. I., 1973, *ApJ*, 182, 809  
 Aerts C., Christensen-Dalsgaard J., Kurtz D. W., 2010, *Asteroseismology*. Springer-Verlag, Berlin  
 Antoci V. et al., 2014, *ApJ*, 796, 118  
 Balmforth N. J., 1992, *MNRAS*, 255, 603  
 Balona L. A. et al., 2011, *MNRAS*, 414, 792  
 Balona L. A., Catanzaro G., Abedigamba O. P., Ripepi V., Smalley B., 2015a, *MNRAS*, 448, 1378  
 Balona L. A., Daszyńska-Daszkiewicz J., Pamyatnykh A. A., 2015b, *MNRAS*, 452, 3073  
 Bouabid M.-P., Dupret M.-A., Salmon S., Montalbán J., Miglio A., Noels A., 2013, *MNRAS*, 429, 2500  
 Breger M., 1970, *ApJ*, 162, 597  
 Carquillat J.-M., Prieur J.-L., 2007, *MNRAS*, 380, 1064  
 Cox A. N., Hodson S. W., King D. S., 1979, *ApJ*, 231, 798  
 De Cat P. et al., 2015, *ApJS*, 220, 19  
 Deal M., Richard O., Vauclair S., 2016, *A&A*, 589, A140  
 Debosscher J., Blomme J., Aerts C., De Ridder J., 2011, *A&A*, 529, A89  
 Ferguson J. W., Alexander D. R., Allard F., Barman T., Bodnarik J. G., Hauschildt P. H., Heffner-Wong A., Tamanai A., 2005, *ApJ*, 623, 585

- Gough D., 1977a, in Spiegel E. A., Zahn J.-P., eds, *Lecture Notes in Physics*, Vol. 71, *Problems of Stellar Convection*. Springer-Verlag, Berlin, p. 15
- Gough D. O., 1977b, *ApJ*, 214, 196
- Grassitelli L., Fossati L., Langer N., Miglio A., Istrate A. G., Sanyal D., 2015, *A&A*, 584, L2
- Grigahcène A. et al., 2010, *ApJ*, 713, L192
- Handler G., Shobbrook R. R., 2002, *MNRAS*, 333, 251
- Henry G. W., Fekel F. C., 2005, *AJ*, 129, 2026
- Holdsworth D. L., 2015, PhD thesis, Keele University
- Holdsworth D. L. et al., 2014, *MNRAS*, 439, 2078
- Hou W. et al., 2015, *MNRAS*, 449, 1401
- Houdek G., Balmforth N. J., Christensen-Dalsgaard J., Gough D. O., 1999, *A&A*, 351, 582
- Jenkins J. M. et al., 2010, *ApJ*, 713, L87
- Kohl K., 1964, *Z. Astrophys.*, 60, 115
- Kurtz D. W., 1976, *ApJS*, 32, 651
- Kurtz D. W., 1978, *ApJ*, 221, 869
- Kurtz D. W., 1989, *MNRAS*, 238, 1077
- Layden A. C., 1994, *AJ*, 108, 1016
- Lenz P., Breger M., 2005, *Commun. Asteroseismol.*, 146, 53
- Lund M. N., Handberg R., Davies G. R., Chaplin W. J., Jones C. D., 2015, *ApJ*, 806, 30
- Luo A.-L. et al., 2015, *Res. Astron. Astrophys.*, 15, 1095
- Michaud G., 1970, *ApJ*, 160, 641
- Murphy S. J., 2014, PhD thesis, Jeremiah Horrocks Institute, Univ. Central Lancashire
- Pollacco D. L. et al., 2006, *PASP*, 118, 1407
- Press W. H., Rybicki G. B., 1989, *ApJ*, 338, 277
- Press W. H., Teukolsky S. A., Vetterling W. T., Flannery B. P., 1992, *Numerical Recipes in FORTRAN. The Art of Scientific Computing*, 2nd edn. Cambridge Univ. Press, Cambridge
- Renson P., Manfroid J., 2009, *A&A*, 498, 961
- Rodríguez E., Breger M., 2001, *A&A*, 366, 178
- Rodríguez E., López-González M. J., López de Coca P., 2000, *A&AS*, 144, 469
- Rogers F. J., Iglesias C. A., 1995, in Adelman S. J., Wiese W. L., eds, *ASP Conf. Ser. Vol. 78, Astrophysical Applications of Powerful New Databases*. Astron. Soc. Pac., San Francisco, p. 31
- Roman N. G., Morgan W. W., Eggen O. J., 1948, *ApJ*, 107, 107
- Smalley B., Kupka F., 1997, *A&A*, 328, 349
- Smalley B. et al., 2011, *A&A*, 535, A3
- Smalley B. et al., 2014, *A&A*, 564, A69
- Smith M. A., 1973, *ApJS*, 25, 277
- Spiegel M. R., Schiller J. J., Srinivasan A., 2001, *Probability and Statistics*. McGraw-Hill, New York
- Tamuz O., Mazeh T., Zucker S., 2005, *MNRAS*, 356, 1466
- Théado S., Alecian G., LeBlanc F., Vauclair S., 2012, *A&A*, 546, A100
- Titus J., Morgan W. W., 1940, *ApJ*, 92, 256
- Turcotte S., Richer J., Michaud G., Christensen-Dalsgaard J., 2000, *A&A*, 360, 603
- Wolff S. C., 1983, *The A-type Stars: Problems and Perspectives*. NASA SP-463, Washington, DC
- Wu Y. et al., 2011, *Res. Astron. Astrophys.*, 11, 924
- Xiong D.-R., Deng L.-C., Wang K., 2015, *Chin. Astron. Astrophys.*, 39, 16
- Zacharias N., Monet D. G., Levine S. E., Urban S. E., Gaume R., Wycoff G. L., 2004, *BAAS*, 36, 1418
- Zhao G., Zhao Y.-H., Chu Y.-Q., Jing Y.-P., Deng L.-C., 2012, *Res. Astron. Astrophys.*, 12, 723

## SUPPORTING INFORMATION

Supplementary data are available at [MNRAS](https://academic.oup.com/mnras) online.

**Table 1.** The results of the search for variability in WASP light curves.

Please note: Oxford University Press is not responsible for the content or functionality of any supporting materials supplied by the authors. Any queries (other than missing material) should be directed to the corresponding author for the article.

This paper has been typeset from a  $\text{\TeX}/\text{\LaTeX}$  file prepared by the author.